Supplementary information for

Promoting photocatalytic nitrogen fixation with alkali metal cations and plasmonic nanocrystals

Tong-An Bu, Yu-Chen Hao, Wen-Yan Gao, Xin Su, Li-Wei Chen, Nan Zhang, An-Xiang Yin*

MOE Key Laboratory of Cluster Science, Beijing Key Laboratory of Photoelectronic/Electrophotonic Conversion Materials, School of Chemistry and Chemical Engineering, Beijing Institute of Technology, Beijing 100081, P. R. China.

*To whom correspondence should be addressed: yin@bit.edu.cn

I. Additional Experimental Details

Materials

P25 TiO_2 (Aeroxide^{TM}) was purchased from Acros. Zinc oxide (ZnO, 99.8%) was purchased from Macklin (China). Silver nitrate ($AgNO_3$, 99.8%), hydrogen tetrachloroaurate(III) ($HAuCl_4$, 98%) and sodium borohydride ($NaBH_4$, 98%) were purchased from Energy Chemical (China). Bismuth (III) nitrate pentahydrate ($Bi(NO_3)_3 \cdot 5H_2O$, 98%), ethylene glycol ($C_2H_6O_2$, 99%), and potassium sulfate (K_2SO_4, 99%) were purchased from Alfa Aesar (USA). Ethanol (CH_3CH_2OH, 98%) was purchased from Beijing Chemical Reagent Co. Ltd. (China). Nessler's reagent and $^{15}N_2$ (99 atom % of ^{15}N) were purchased from Aladdin (China). Dimethyl sulfoxide-d6 (99.9 atom % D), sodium hydroxide (NaOH, 98%), sodium hypochlorite (NaClO), sodium nitroprusside dihydrate ($C_5FeN_6Na_2O \cdot 2H_2O$, 99%) and sodium salicylate ($C_7H_5NaO_3$) were purchased from Sigma Adrich (USA). All the chemicals were used as received without any further purification. The water (18 MΩ cm) used in all experiments was prepared by passing through an ultra-pure purification system.

Preparation of Au-nanocrystal-decorated P25 (Au/P25) catalysts

In a typical synthesis, 0.1 g of P25 was fully dispersed in 20 mL of ultra-pure water and sonicated for 2 h. Then, 2 mL of 10.0 mM hydrogen tetrachloroaurate ($HAuCl_4$) solution was added into the dispersion. The mixture solution was then vigorously stirred at room temperature for 12 hours and sonicated for another 15 min. After that, 5 mL of ethanol solution containing 0.1 M $NaBH_4$ was injected into the mixture solution dropwise under vigorous stirring (1500 rpm min^{-1}). After another 1 h of continuous stirring, the final products were collected by centrifuge, washed with ethanol and water for several times, and dried in a vacuum oven.

Preparation of Ag-nanocrystal-decorated P25 (Ag/P25) catalysts

The preparation of Ag/P25 was similar to that of Au/P25, except that silver nitrate ($AgNO_3$) was used instead of $HAuCl_4$ as precursors.

Preparation of BiOBr nanosheet

BiOBr was prepared with a modified procedure reported previously[1]. In a typical synthesis, 3 mmol of $Bi(NO_3) \cdot 5H_2O$ was added into 40 mL of ethylene glycol solution containing 3 mmol of KBr. The mixture solution was vigorously stirred for 2 h and sonicated for another 15 min. The solution was transferred into a 50 mL Teflon-lined stainless steel autoclave, which was put into an oven at 160 ^{o}C for 12 h and then cooled to room temperature by air. The final products were collected by centrifuge, washed with ethanol for several times, and dried in a vacuum oven.

Structure and composition characterization

Powder X-ray diffraction (XRD) was performed on a Rigaku MiniFlex 600 diffractometer with a Cu-Kα X-ray radiation source ($\lambda = 0.154056$ nm) at the scan rate of 8° min^{-1}. X-ray photoelectron spectroscopy (XPS) measurement was obtained by a Thermo VG ESCALAB-250 system with Al-Kα and Mg-Kα sources operated at 15 kV.

Transmission electron microscopy (TEM) and high-resolution TEM (HRTEM) studies were performed on a JEM-2100 (JEOL, Japan) transmission electron microscope operating at 200 kV. At least 200 nanoparticles were counted for the size-distribution histograms.

Photocatalysis tests

A 300 W Xe lamp (CEL-S500, Beijing China Education Au-light Co., Ltd.) was used as the light source and the light intensity was adjusted to 100 mW cm^{-2}. For typical tests, 5 mg of photocatalyst (e.g. P25, Au/P25, Ag/P25, ZnO, and BiOBr) were added into a quartz reactor containing 50 mL of aqueous solutions. N_2 was bubbled into the reactor with a flow rate of 60 mL min^{-1} before and during the reactions. A 400 nm cut-on filter was used for photocatalysis reactions under visibile light.

In the process of reaction, a certain volume of suspension was extracted from the reactor every 15 min and centrifuged immediately to remove the catalysts. For photocatalytic reactions without any sacrificial reagents, the produced ammonia was quantificated with both the Nessler's reagent[1] and the indophenol-blue method[2]. For photocatalytic reactions using methanol as sacrificial reagents, only the indophenol-blue method was used since methanol would be oxidized to carbonyl compounds and interfere the tests with Nessler's reagents[3].

Quantification of NH_3 using Nessler's reagents

The produced ammonia was quantified through colorimetric method using Nessler's reagents[1]. All test solutions were incubated under dark conditions at 25 °C for 20 min before UV-vis measurements. The absorbance at 420 nm for each coloration solution was measured by the UV-vis spectrophotometer (Shimadzu, UV-2600). A series of reference solutions with suitable NH_4Cl concentrations was made to measure their UV-vis absorbance at 420 nm and to plot a calibration curve (ammonium concentration versus absorbance) (Supplementary Fig. 6). The concentrations of ammonia in the extracted reaction solutions could be obtained through the calibration curve.

Quantification of NH_3 using the indophenol-blue method

The quantity of the produced ammonia could also be mesured with the indophenol-blue method[2]. All test solutions were incubated under dark conditions at 25 °C for 2 h before UV-vis measurements. The absorbance at 670 nm for each coloration solution was measured by the UV-vis spectrophotometer (Shimadzu, UV-2600). A series of reference solutions with suitable NH_4Cl concentrations was made to measure their UV-vis absorbance at 670 nm for plotting a calibration curve (ammonium concentration versus absorbance) (Supplementary Fig. 7). The concentrations of ammonia in the extracted reaction solutions could be obtained through the calibration curve.

Nuclear magnatic resonance (NMR) measurements and Isotope-labelling experiments

NMR measuremenrs were also used to identify the produced ammonia[4]. After photocatalytic nitrogen reduction reactions, a certain amount of aliquot (0.5 mL) was extracted from the quartz reactor and then mixed with 0.1 mL of 20% DMSO-d_6 (Sigma). NMR measurements were then performed on a Bruker Ascend 700-MHz system. For isotopelabelled experiments, $^{15}N_2$ (99 atom%) was bubbled into an air-tight reactor with a flow rate of 20 mL min^{-1} using a gas-circulation pump. NMR measurements were them performed following the aforementioned procudure.

Quantification of H_2

An air-tight reaction cell with a gas-circulation system attached to an on-line gas chromatography (Shimadzu GC-2014C, with a MS-13X packed column and a TCD detector) was used to monitor the amount of H_2 generated during the photocatalytic reaction. The flow rate of N_2 was 20 mL min^{-1}. The amount of produced ammonia was also measured with Nessler's reagents.

Quantum efficiency calculation

Typically, photocatalytic reactions were performed for 10 hours (*T*) under irradiation of the Xe lamp with band-pass filters for centain wavelengths (*λ*). The irradiation area (*S*) was set to 28.26 cm^2. The irradiation intensity (*E*) was determined by an ILT950 spectroradiometer (International Light Technologies). The number of incident photons (*N*) could be calculated by equation (1) (*ref.* 5)

$$N = \frac{EST\lambda}{hc} \qquad (1)$$

where $h = 6.626 \times 10^{-34}\,J\,s$, $c = 3 \times 10^{8}\,m\,s^{-1}$, and $T = 10\,h \times 3600\,s\,h^{-1} = 36000\,s$.

The apparent quantum efficiency (AQE) is calculated from equation (2).

$$AQE = \frac{3 \times Number(NH_3\,molecules)}{Number(incident\,photons)} \times 100\% \qquad (2)$$

II. Supplementary data

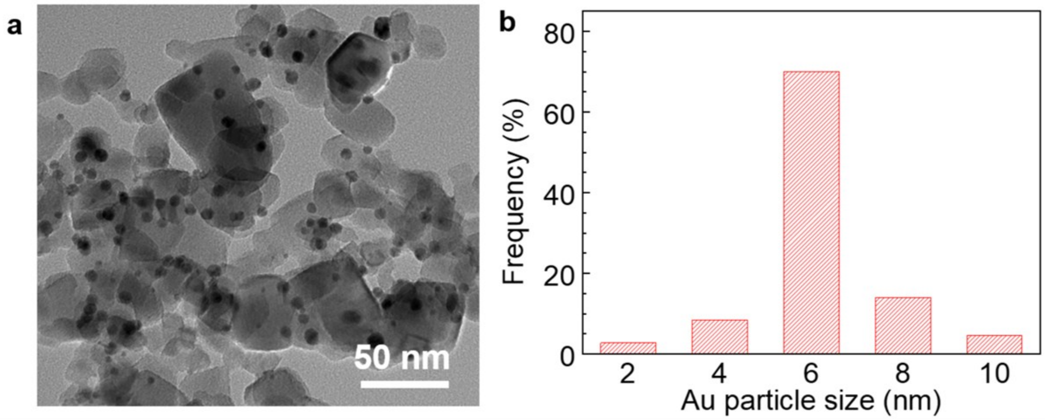

Fig. S1 Transmission electron microscopy (TEM) images (a) and histograms for the size distributions of Au nanocrystals (AuNCs) (b) for Au/P25. The size distributions for more than 200 AuNCs are (5.78 ± 1.14) nm.

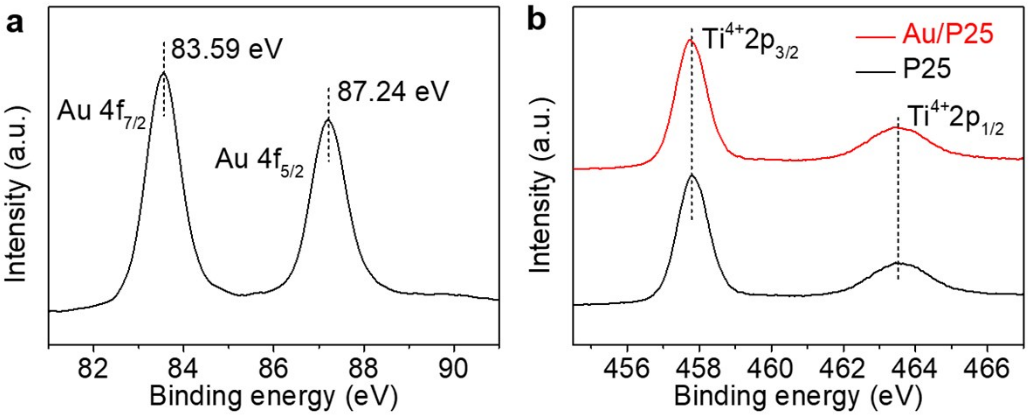

Fig. S2 High-resolution X-ray photoelectron spectroscopy (XPS) profiles for (a) Au 4f of Au/P25 and (b) Ti 2p of Au/P25 and P25, respectively.

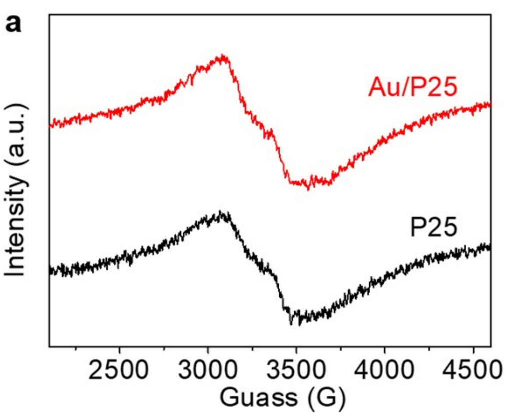

Fig. S3 (a) Electron paramagnetic resonance (EPR) spectra of P25 and Au/P25, (b) Nitrogen-sorption on P25 and Au/P25.

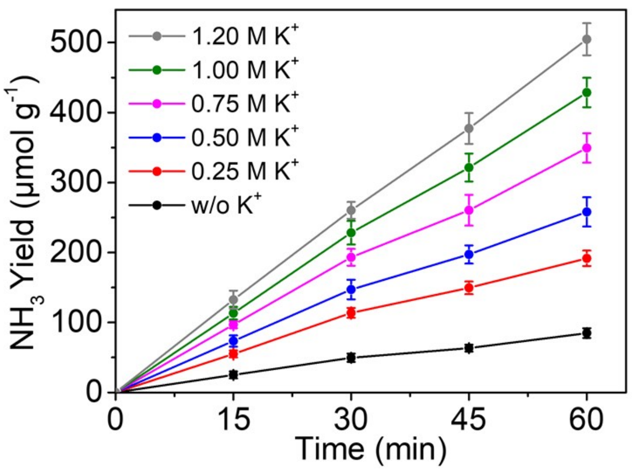

Fig. S4 Ammonia yield on Au/P25 under UV-vis irradiation in solutions with different concentrations of potassium cations. The error bars indicate the standard deviation of three independent samples.

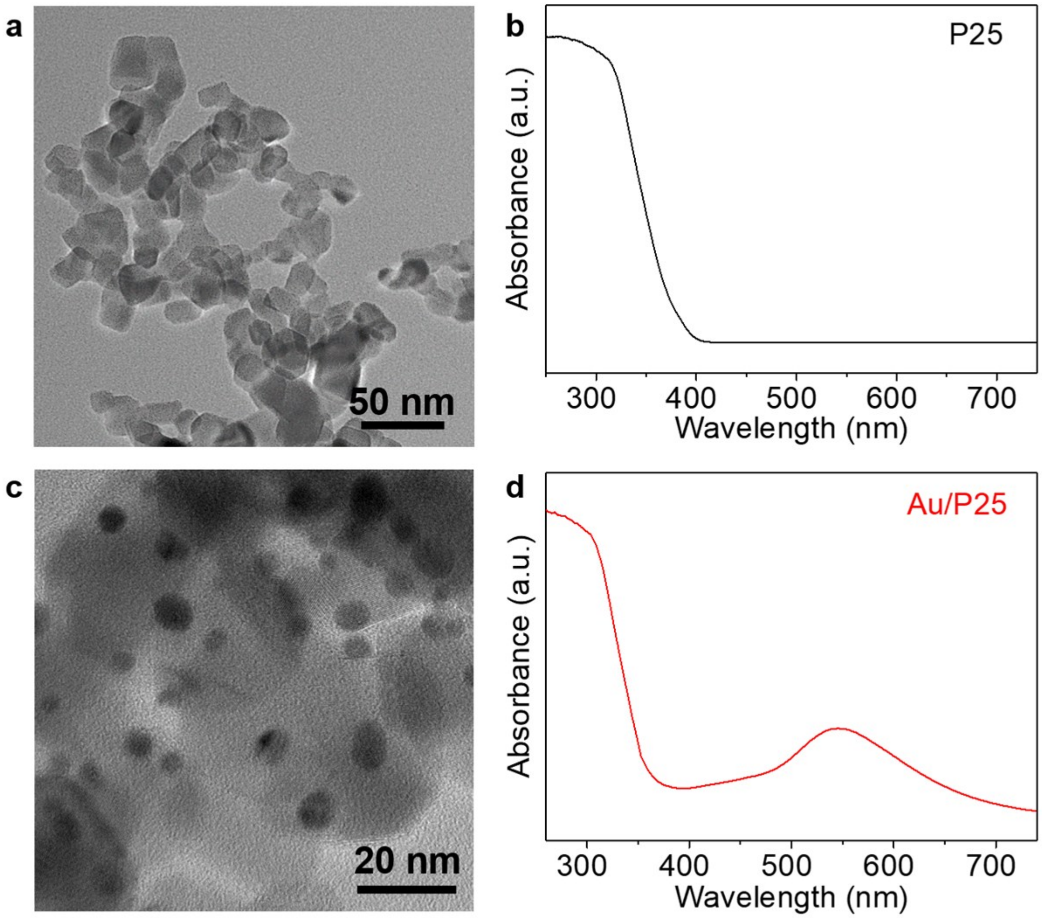

Fig. S5 Transmission electron microscopy (TEM) images and UV-vis spectra for P25 and Au/P25 after photocatalytic reactions. (a, b) TEM image and UV-vis spectrum for P25 after 10 runs (1 h per run) of photocatalytic tests. (c, d) TEM image and UV-vis spectrum for Au/P25 after 10 runs (1 h per run) of photocatalytic tests.

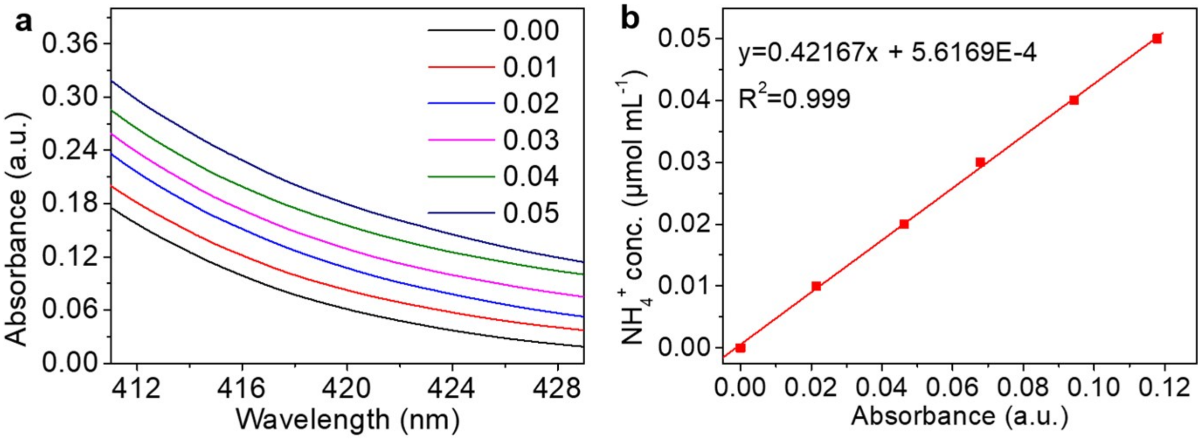

Fig. S6 UV-vis spectra and calibration curve for ammonium quantification using the Nessler's reagents. (a) UV-vis spectra for standard NH_4^+ solutions with the concentration of 0.00, 0.01, 0.02, 0.03, 0.04, and 0.05 μmol mL^{-1}, respectively. (b) The calibration curve for ammonium quantification (NH_4^+ concentration versus absorbance at 420 nm).

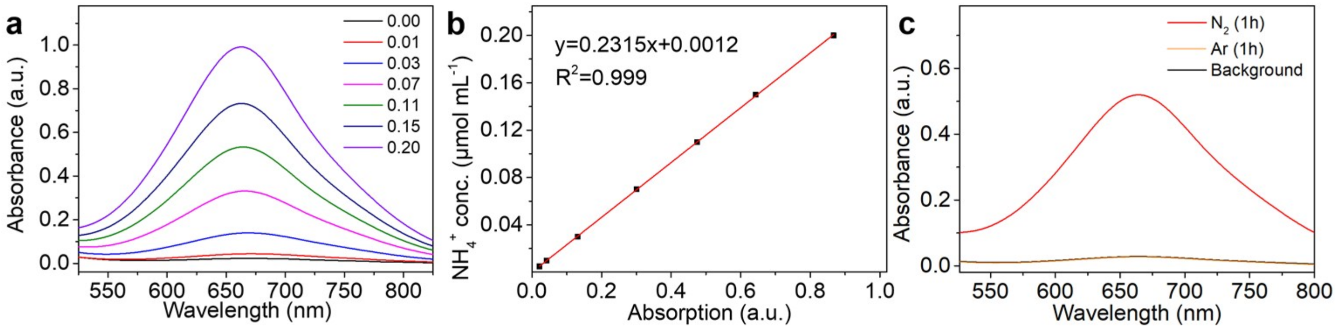

Fig. S7 UV-vis spectra and calibration curve for ammonium quantification using the indophenol-blue method. (a) UV-vis spectra for standard NH_4^+ solutions with the concentration of 0.00, 0.01, 0.03, 0.07, 0.11, 0.15 and 0.20 µmol mL^{-1}, respectively. (b) The calibration curve for ammonium quantification (NH_4^+ concentration versus absorbance at 670 nm). (c) UV-vis spectra for (1) the pristine mixture solution of K_2SO_4 (0.50 mol L^{-1}) and methanol (1.0 mol L^{-1}) (black line, background), (2) the mixture solution after 1 h of photocatalysis reaction with Ar bubbling (orange line), and (3) the mixture solution after 1 h of photocatalysis reaction with N_2 supply (red line).

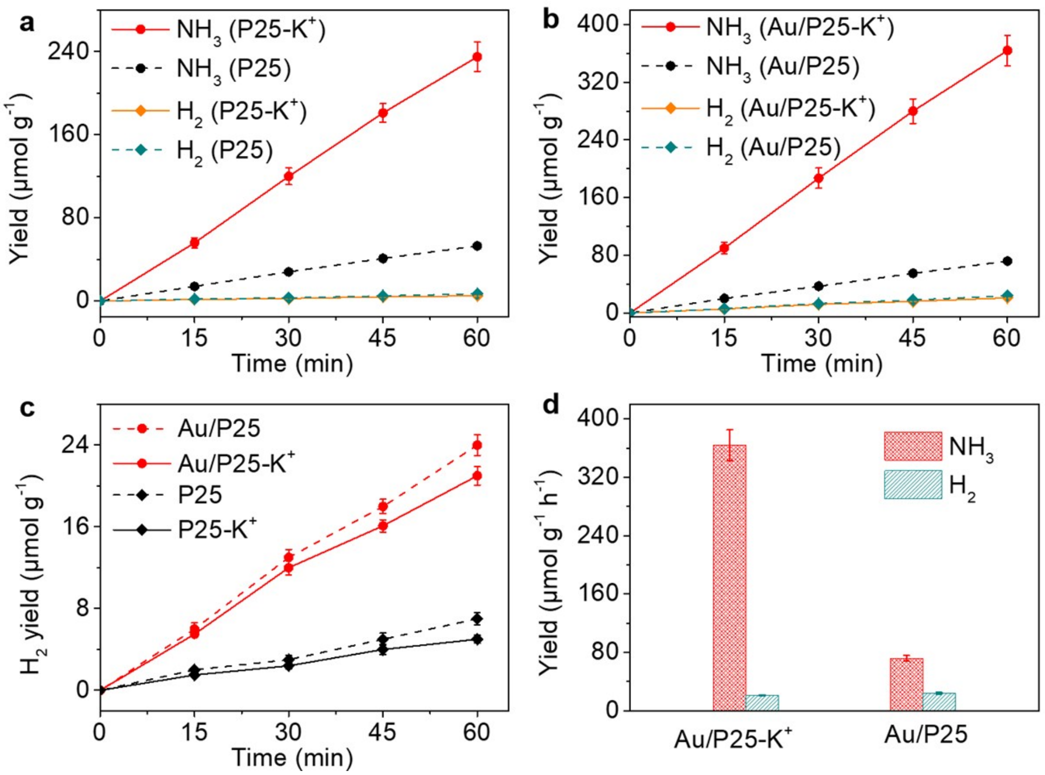

Fig. S8 Evolution rates for NH$_3$ and H$_2$ on Au/P25 and P25. (a, b) Ammonia and hydrogen evolution rates on (a) P25 and (b) Au/P25 under UV-vis irradiation in solutions with/without potassium cations (1.0 mol L^{-1}), respectively. (c) H$_2$ evolution rate on Au/P25 and P25 under UV-vis irradiation in solutions containing 0 and 1 mol L^{-1} of K$^+$, respectively. (d) Comparison of NH$_3$ and H$_2$ evolution rates on Au/P25 in solutions with/without potassium cations (1.0 mol L^{-1}), respectively. The error bars indicate the standard deviation of three independent samples.

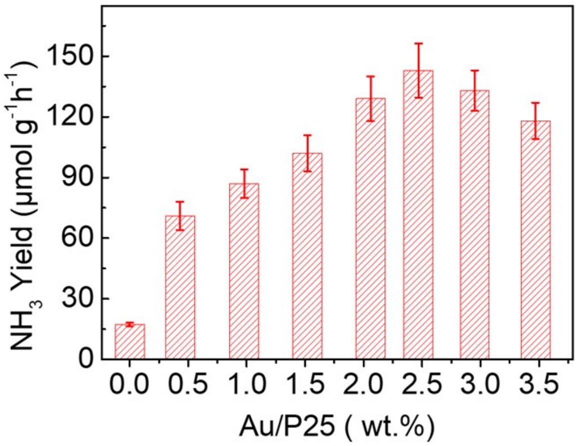

Fig. S9 Ammonia evolution rates on Au/P25 with different Au mass loadings under visiable light in solutions containing 1.0 mol L^{-1} of potassium cations. The error bars indicate the standard deviation of three independent samples.

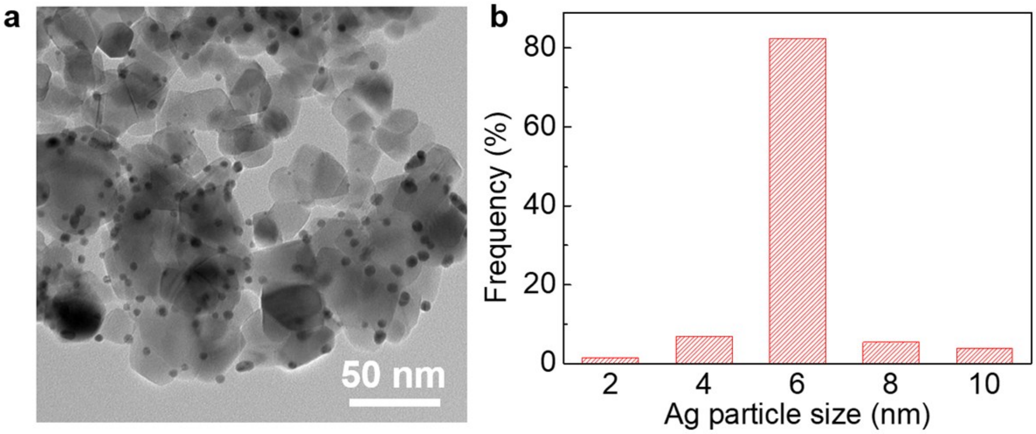

Fig. S10 Ag/P25 samples. (a) Transmission electron microscopy (TEM) image and (b) histograms for the size distributions of Ag nanocrystals (AgNCs) for Ag/P25. The size distributions for more than 200 AgNCs are (6.18 ± 1.21) nm.

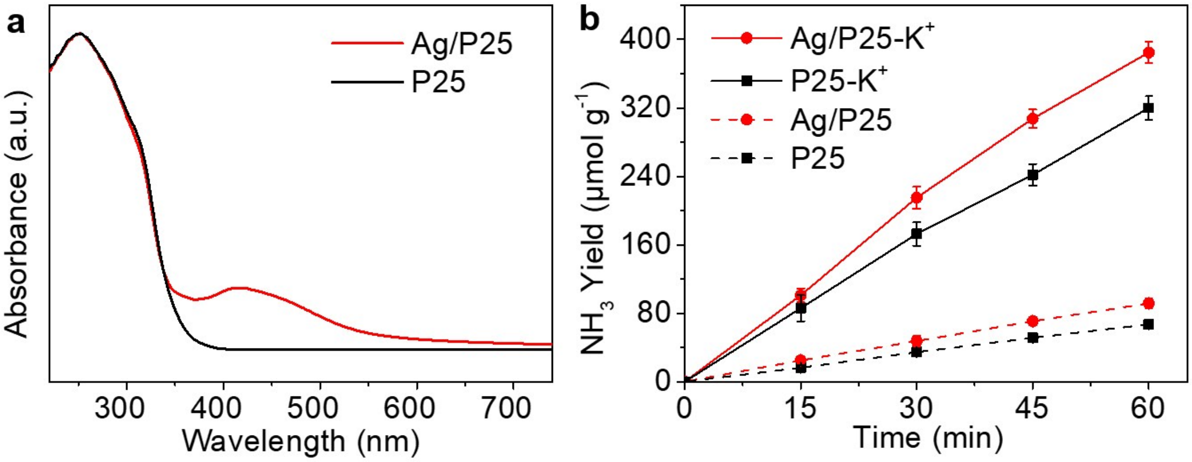

Fig. S11 PNRR on Ag/P25. (a) UV-vis absorbance for Ag/P25 (red) and P25 (black). (b) Ammonia yield on Ag/P25 and P25 under UV-vis irradiation in solutions containing 0 and 1.0 mol L^{-1} of potassium cations, respectively. The error bars indicate the standard deviation of three independent samples.

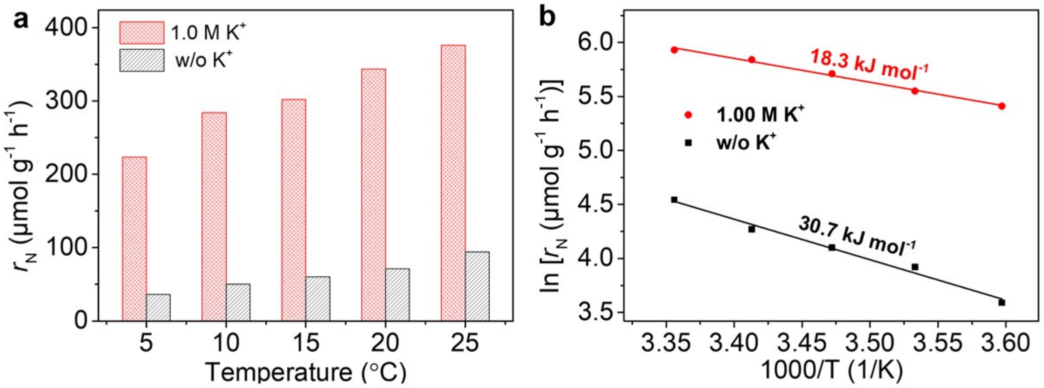

Fig. S12 Apparent activation energy (*E*a) measurement for PNRR on P25. (a) Ammonia evolution rates on P25 under UV-vis irradiation in solutions with/without potassium cations (1.0 mol L^{-1}) at different temperatures ranging from 5 to 25 °C. (b) Corresponding apparent *E*a for photocatalyitc nitrogen reduction on P25 in solutions with/without potassium cations (1.0 mol L^{-1}).

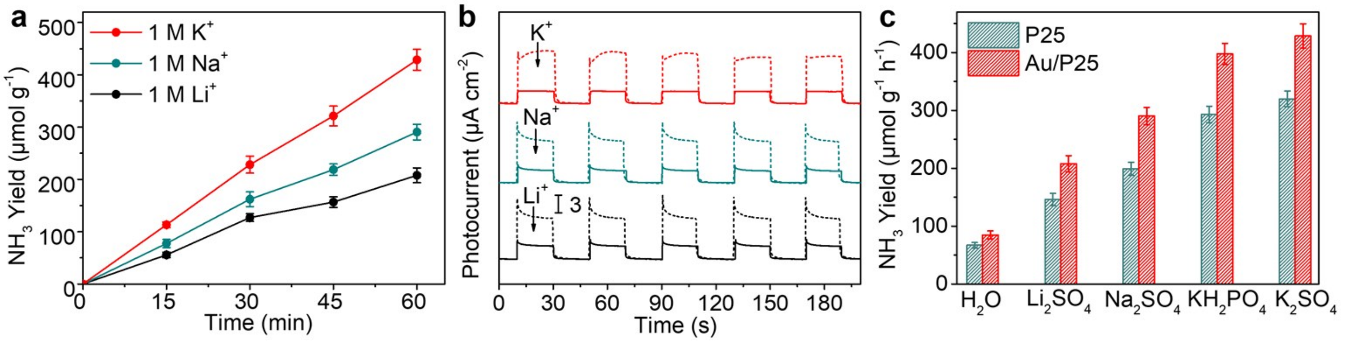

Fig. 13 PNRR on Au/P25 in solutions with Li^+, Na^+ and K^+ cations. (a) Ammonia production on Au/P25 under UV-vis illumination in solutions with 1.0 mol L^{-1} of K^+ (red), Na^+ (cyan), and Li^+ (black), respectively. (b) Photocurrents on Au/P25 catalysts in Ar (dotted lines) or N_2-saturated (solid lines) solutions containing 1.0 mol L^{-1} of K^+ (red), Na^+ (cyan), and Li^+ (black), respectively. (c) Ammonia evolution on P25 and Au/P25 under UV-vis light in solutions of H_2O, 0.50 mol L^{-1} Li_2SO_4, 0.50 mol L^{-1} Na_2SO_4, 1.0 mol L^{-1} KH_2PO_4, and 0.50 mol L^{-1} K_2SO_4, respectively. The error bars indicate the standard deviation of three independent samples.

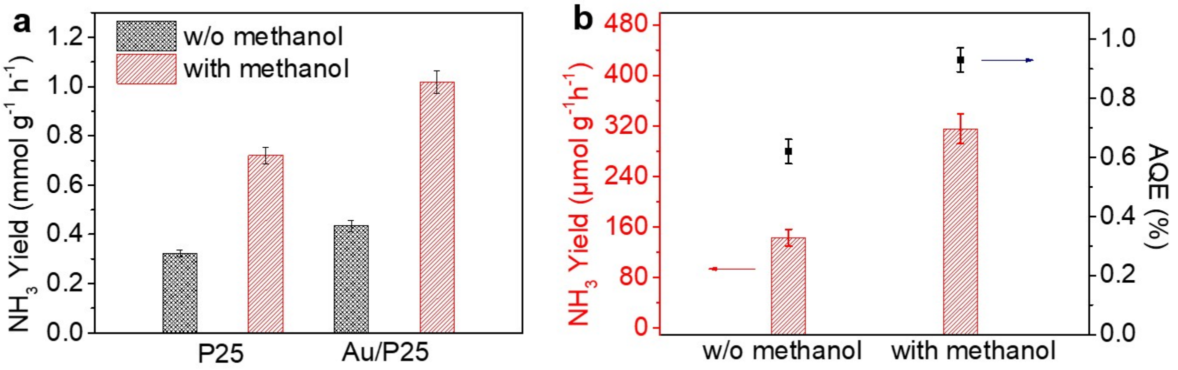

Fig. S14 PNRR on P25 and Au/P25 with methanol as hole scavenger. (a) Ammonia yields on P25 and Au/P25 in solutions with/without methanol (1 mol L^{-1}) under UV-Vis illumination. (b) Ammonia yields on P25 and Au/P25 in solutions with/without methanol (1 mol L^{-1}) under visible light (left axis) and the corresponding apparent quantum efficiency (AQE, right axis) at 550 nm. The error bars indicate the standard deviation of three independent samples.

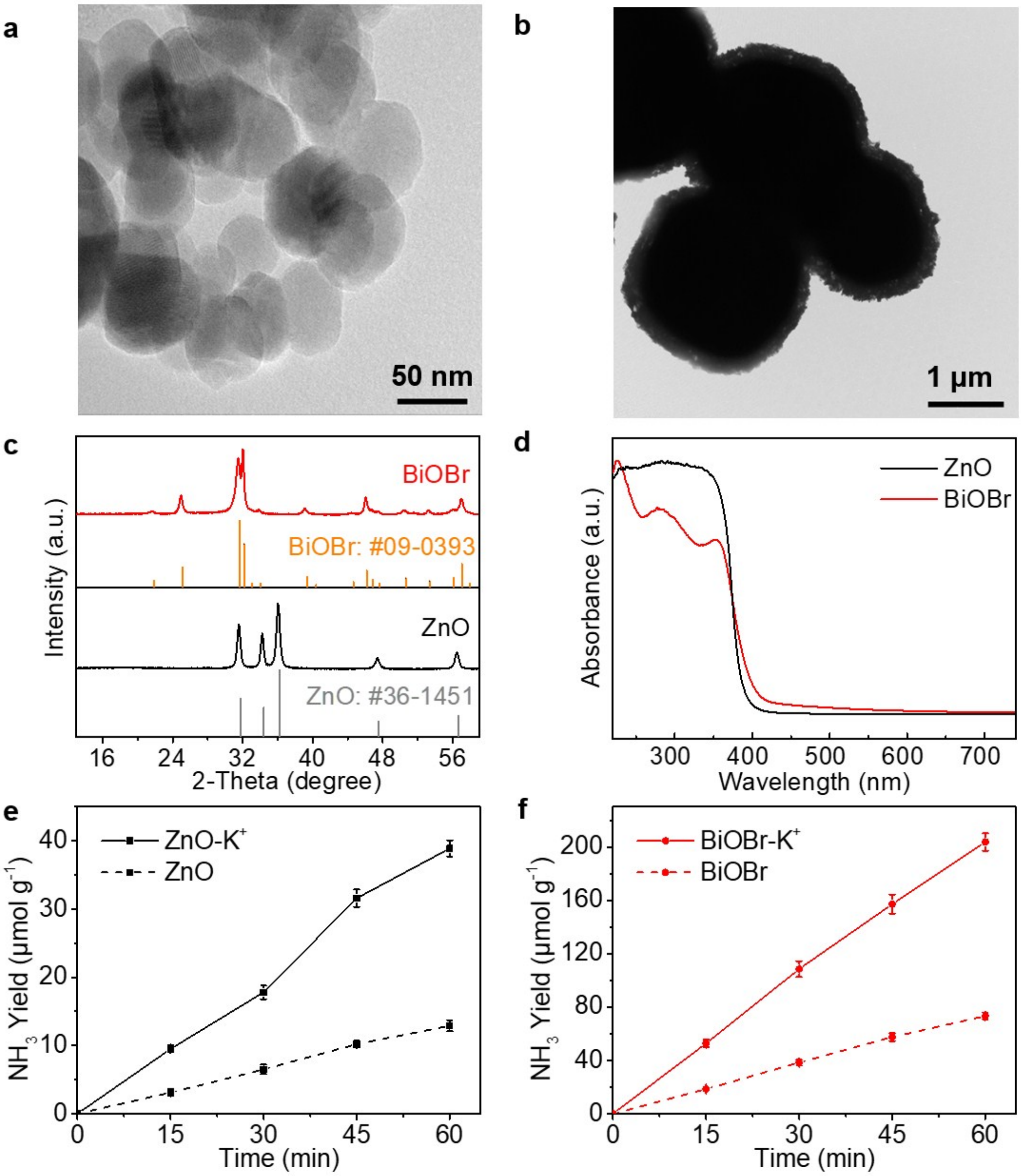

Fig. S15 PNRR on ZnO and BiOBr. (a, b) TEM images for (a) ZnO and (b) BiOBr, respectively. (c) XRD patterns and (d) UV-vis spectra for ZnO and BiOBr catalysts. (e, f) Ammonia yield on (e) ZnO and (f) BiOBr under UV-vis irradiation in solutions with 0 and 1.0 mol L^{-1} of potassium cations, respectively.

Table S1 Pepresentative works on photocatalytic nitrogen fixation.

Catalysts	**Light source**	**Scavenger**	**AQE (%)**	**Yield (μmol g^{-1}h^{-1})**	**Ref.**
BiOBr-001-OVs	full spec.	/	0.23@420 nm	223.3	1
	> 420 nm	/		104.2	1
Au/TiO$_2$-OVs	white light	methanol	0.82@550 nm	187.1	2
	> 420 nm	methanol		130.5	2
Bi$_5$O$_7$Br	> 400 nm	/	2.3@420 nm	1380	4
MoS$_2$	full spec.	/		325	6
Bi$_5$O$_7$I {001}	280–800 nm	methanol	5.1@365 nm	11.15	7
TiO$_2$-OVs	full spec.	2-propanol	0.7@350 nm	0.73	8
CuCr-LDH	> 400 nm	/	0.10@500 nm	73.9	9
Ru/TiO$_2$	full spec.	methanol		29.4	10
Fe-dopedTiO$_2$	full spec.	/		11.58	11
Fe@3Dgraphene	full spec.	/		24	12
C-WO$_3$·H$_2$O	full spec.	/		63.55	13
Pt-CdS	full spec.	/		16.3	14
Fe$_2$O$_3$	full spec.	methanol		10.0	15
BiO quantum dots	full spec.	/		1226	16
P25	**full spec.**	**/**	**0.06@380 nm**	**67**	**This work**
	> 400 nm	**/**	**~0@400 nm; ~0@550 nm**	**0.14**	**This work**
P25–K$^+$	**full spec.**	**/**	**0.32@380 nm**	**320**	**This work**
	> 400 nm	**/**	**0.03@400 nm; ~0@550 nm**	**17.3**	**This work**
Au/P25	**full spec.**	**/**	**0.04@400 nm**	**84.8**	**This work**
	> 400 nm	**/**	**0.13@550 nm**	**21.0**	**This work**
Au/P25–K$^+$	**full spec.**	**/**	**0.34@400 nm**	**428.7**	**This work**
	> 400 nm	**/**	**0.62@550 nm**	**143**	**This work**
Au/P25–K$^+$	**full spec.**	**methanol**		**1020**	**This work**
	> 400 nm	**methanol**	**0.93@550 nm**	**315**	**This work**

References

1 H. Li, J. Shang, Z. H. Ai, L. Z. Zhang, *J. Am. Chem. Soc.* 2015, **137**, 6393–6399.

2 J. H. Yang, Y. Z. Guo, R. B. Jiang, F. Qin, H. Zhang, W. Z. Lu, J. F. Wang, J. C. Yu, *J. Am. Chem. Soc.* 2018, **140,** 8497–8508.

3 X. Gao, Y. J. Wen, D. Qu, L. An, S. L. Luan, W. S. Jiang, X. P. Zong, X. Y. Liu, Z. C. Sun, *ACS Sustain. Chem. Eng.* 2018, **6**, 5342–5348.

4 S. Y. Wang, X. Hai, X. Ding, K. Chang, Y. G. Xiang, X. G. Meng, Z. Yang, H. Chen, J. H. Ye, *Adv. Mater*. 2017, **29**, 1701774.

5 J. Liu, Y. Liu, N. Y. Liu, Y. Z. Han, X. Zhang, H. Huang, Y. Lifshitz, S. T. Lee, J. Zhong, Z. H. Kang, *Science* 2015, **347,** 967–970.

6 S. M. Sun, X. M. Li, W. Z. Wang, L. Zhang, X. Sun, *Appl. Catal. B.* 2017, **200**, 323–329.

7 Y. Bai, L. Q. Ye, T. Chen, L. Wang, X. Shi, X. Zhang, D. Chen, *ACS Appl. Mater. Inter.* 2016, **8**, 27661–27668.

8 H. Hirakawa, M. Hashimoto, Y. Shiraishi, T. Hirai, *J. Am. Chem. Soc.* 2017, **139**, 10929–10936.

9 Y. F. Zhao, Y. X. Zhao, G. I. N. Waterhouse, L. R. Zheng, X. Z. Cao, F. Teng, L. Z. Wu, C. H. Tung, D. O. Hare, T. R. Zhang, *Adv. Mater.* 2017, **29**, 1703828.

10 K. T. Ranjit, T. K. Varadarajan, B. Viswanathan, *J. Photochem. Photobiol. A: Chem.* 1996, **96**, 181–185.

11 G. N. Schrauzer, T. D. Guth, *J. Am. Chem. Soc.* 1977, **99**, 7189–7193.

12 Y. H. Lu, Y. Yang, T. F. Zhang, Z. Ge, H. C. Chang, P. S. Xiao, Y. Y. Xie, L. Hua, Q. Y. Li, H. Li, B. Ma, N. J. Guan, Y. F. Ma, Y. S. Chen, *ACS Nano* 2016, **10**, 10507–10515.

13 X. M. Li, W. Z. Wang, D. Jiang, S. M. Sun, L. Zhang, X. Sun, *Chem. Eur. J.* 2016, **22**, 13819–13822.

14 H. Miyama, N. Fujii, Y. Nagae, *Chem. Phys. Lett.* 1980. **74**, 523–524.

15 M. M. Khader, N. N. Lichtin, G. H. Vurens, M. Salmeron, G. A. Somorjai, *Langmuir* 1987, **3**, 303–304.

16 S. M. Sun, Q. An, W. Z. Wang, L. Zhang, J. J. Liu, W. A. Goddard III, *J. Mater. Chem. A* 2017, **5**, 201–209.